Proceedings of the Twenty-eighth (2018) International Ocean and Polar Engineering Conference
Sapporo, Japan, June 10-15, 2018

ISBN 978-1-880653-87-6; ISSN 1098-6189

www.isope.org

Thermomechanical Analysis of Composites Under Shock Load Using Peridynamics

*Yan Gao, Selda Oterkus**
Department of Naval Architecture, Ocean and Marine Engineering, University of Strathclyde.
Glasgow, United Kingdom

ABSTRACT

Composite structures have been increasingly used in marine industries because of their high performance. During their service time, they may be exposed to extreme loading conditions such as underwater explosions. Both thermal loading effects on deformation and deformation effects on temperature need to be taken into consideration in the numerical simulations. Therefore, a thermomechanical analysis is conducted in a fully coupled manner, in order to investigate the thermal and mechanical responses of composite materials under explosion loads. In this study, the peridynamics theory is used for failure analyses of composite structures

KEY WORDS: Peridynamics; thermomechanical; composites; shock load.

INTRODUCTION

In recent years, composites have been employed in a variety of applications in marine structures. Their high performances such as high strength-to-weight ratios and reduced maintenance requirements give them a bright future in marine industries. In addition, these characteristics have garnered them recent attention as effective materials in military applications (LiVolsi, 2014). Military structures are frequently exposed to extreme loads in the field or at sea, thus the extreme loading conditions need to be considered in their design state without any compromises from their weights (Diyaroglu, 2016). In the realm of varies types of extreme loadings, the explosive loading or blast loading is a typical and critical one, which draws a lot of attentions in marine composites research. However, different types of material, i.e. fibre and matrix, are involved in the construction process of composites, making the properties of composites materials being rather complex. What's more, the highly nonlinear response of composites under explosion loads makes the analysis being more challenging. Therefore, various studies concentrate on this issue with the increasing abilities of modern computers.

In the safety analysis of composite marine structures, the failure mechanism study, or more specifically speaking, the crack propagation prediction is a critical factor. The investigation of this type of problem generally falls into three categories: analytical method, experimental study, and numerical simulation. Analytical method could provide relatively faster solutions compared to the other two methodologies. Hence, it is generally utilized in the initial design state of the composite marine structures without any computational cost. Librescu and Nosier (1990) developed a composite model which incorporated transverse shear deformation and transverse normal stress. Later on, Librescu et al. (2004) addressed the problem of the dynamic response of sandwich flat panels exposed to blast loadings analytically. Compared to the analytical method, the experimental studies may provide more information and give more intuitive senses. There are mainly two types of blast tests, i.e. in air and underwater. In comparison with the underwater tests on full-scale structures, laboratory tests have many advantages, for example, lower cost and easier implementation (Hall, 1989). In addition, scaling techniques are necessary to extend the damage parameters from the specimen level can be extended to the structural level (Rajendran, 2008; Rajendran et al., 2007). As to the third method, the numerical simulation method develops rapidly in recent years because of the increasing computer computing abilities. Dobyns (1981) conducted an analysis of simply-supported orthotropic plates subjected to static and dynamic loads. Batra and Hassan (2008) adopted the finite element method (FEM) to analyse the mechanical responses of several fibre-reinforced composite layers under explosion loading conditions. Leblanc and Shukla (2010) investigated the damage evolution and dynamic response of an E-Glass/Epoxy composite material with an underwater explosive loading condition. Numerical simulation was implemented by utilizing the commercially available LS-DYNA finite element code. And the simulation results were compared with the ones obtained from the experiments. Kazancı (2016) conducted a review on the response of blast loaded laminated composite plates.

An explosion is defined as a rapid release of energy in a short period (Langdon et al., 2017). Therefore, the composite materials may experience high strain rates once the explosive loads are imposed. Consequently, because of the high strain rates, high temperature changes can be induced within a short period through the coupling effects. When

smart composite materials are employed for condition monitoring of critical systems in a ship (Ramakrishnan et al., 2016), the effect of temperature change is unneglectable. Thus, fully coupled analyses which include the bidirectional coupling effects between thermal and mechanical fields are required in these situations. There are many academic achievements in published literatures regarding the fully coupled analyses of composite materials. Rao and Sinha (1997) dealt with the coupled thermo-structural analysis of composites beams using finite element method (FEM), presenting different results from uncoupled analyses. Moreover, the coupled thermoelastic response of a composite plate subjected to thermal shocks was studied by Mukherjee and Sinha (1996) using FEM. Khan et al. (2011) compared the temperature profiles from different FE models in the thermomechanical analyses of composites. Comparatively, boundary element method (BEM) was adopted by Kögl and Gaul (2003) to investigate the coupling effect of composites. In conclusion, the grid-based methods have been widely adopted and deeply studied in the realm of thermoelasticity for composites.

Considering the fact that explosive loadings generally give rise to high level failures and fractures in marine composite structures, classical mechanics which are generally utilized by grid-based methods meets some challenges. The classical theory of solid mechanics relies on partial differential equations. Hence, singular stress and strain are created which are not physical. Therefore, the classical continuum mechanics (CCM) contains inherent limitations for the problems involving discontinuities. Some remedies have been provided within the realm of CCM, i.e. Cohesive Zone Elements (CZE) and eXtended Finite Element Method (XFEM). However, these special techniques are not always satisfactory because of the need for supplemental relations related with crack growth (Silling and Bobaru, 2005). On the other hand, Peridynamics (PD), an alternative approach for failure analyses, is proposed (Silling and Bobaru, 2005) and developed (Silling et al., 2007) quickly in recent years. PD falls into the category of non-local theory. And it utilizes the integration form of equation of motion instead of the differential form adopted in CCM. Consequently, it remains valid even at the places where discontinuities emerge, making damages initiate and propagate spontaneously (Oterkus and Madenci, 2011). In this aspect, the PD theory overcomes the weakness of the CCM. PD has been successfully applied on the issue of thermoelasticity. Oterkus et al. (2014b) applied the PD theory on thermal diffusion problems. Good agreements were obtained between PD predictions and analytical solutions. Then Oterkus et al. (2014a) generalized their thermal model in a fully coupled thermomechanical manner. The coupling effects both on thermal and deformation fields were taken into consideration. Further, the fully coupled thermomechanical PD model was developed from isotropic materials into composite materials (Oterkus and Madenci, 2014).

In this study, a fully coupled thermomechanical analysis is conducted for the problem of composite materials subjected to an underwater explosive load. Firstly, the approach for composites materials modelled by the PD theory is briefly explained. Subsequently, a numerical simulation of a laminated composite under an explosive loading is implemented in a fully coupled manner. Then the damage evolutions of the composite are predicted and compared with experimental results. In addition, the temperature distributions predictions are also investigated.

PERIDYNAMIC THEORY

In this section, some basic aspects of the PD theory which is proposed by Silling and Askari (2005) are briefly explained. As shown in Fig. 1, in the body of R, the material points, $\mathbf{x}$, only interacts with other material points within the region H through prescribed response functions. The radius of H is called horizon and denoted by δ. The other material points within H denoted as $\mathbf{y}$ are called the family members of point $\mathbf{x}$. The relative position vector in the reference configuration from $\mathbf{x}$ to $\mathbf{y}$ is called a bond, denoted $\boldsymbol{\xi} = \mathbf{y} - \mathbf{x}$. In the deformed configuration, the relative displacement is set as $\boldsymbol{\eta} = \mathbf{u}(\mathbf{y}) - \mathbf{u}(\mathbf{x})$, where $\mathbf{u}$ represents the displacement vector. If the stretch between two points is defined as

$$s = \frac{|\boldsymbol{\eta} + \boldsymbol{\xi}| - |\boldsymbol{\xi}|}{|\boldsymbol{\xi}|} \tag{1}$$

then the equation of motion in PD theory is

$$\rho(\mathbf{x})\ddot{\mathbf{u}}(\mathbf{x}, t) = \int_H \mathbf{f}(\boldsymbol{\xi}, \boldsymbol{\eta}, t) dV + \mathbf{b}(\mathbf{x}, t) \tag{2}$$

In the above equation, $\rho(\mathbf{x})$ is the density of point $\mathbf{x}$. $\ddot{\mathbf{u}}(\mathbf{x},t)$ is the acceleration of $\mathbf{x}$ at time t. $\mathbf{f}(\boldsymbol{\xi}, \boldsymbol{\eta}, t)$ is the corresponding PD force between $\mathbf{x}$ and $\mathbf{y}$. $\mathbf{b}(\mathbf{x}, t)$ is body force in the collective configuration. The definition of PD force is

$$\mathbf{f}(\boldsymbol{\xi}, \boldsymbol{\eta}, t) = c(s - \alpha T_{avg}) \frac{\boldsymbol{\xi} + \boldsymbol{\eta}}{|\boldsymbol{\xi} + \boldsymbol{\eta}|} \tag{3}$$

in which α is the linear thermal expansion coefficient of the material, T_{avg} is the average temperature of point $\mathbf{x}$ and $\mathbf{y}$. c is the PD constant parameter.

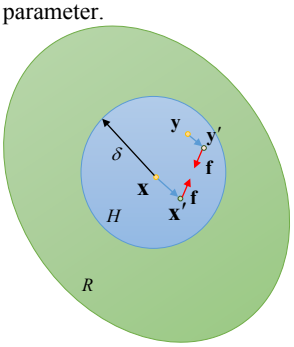

Fig. 1 PD illustration sketch

The locality of interactions depends on the horizon; thus the classical elastic mechanics could be considered as a limiting case of PD theory when the horizon approaches zero. The PD theory is well suited for modelling cracks because of its intrinsic non-local property and the integration form of equations (Silling et al., 2010). As the bond between two points ceases, a crack is initiated and the crack surface is created. At the same time, the integral equation still remains valid. The breakage of a bond is triggered once the stretch exceeds a critical stretch value, s_0. Therefore, a history dependent function, $\mu(\boldsymbol{\xi}, t)$, is introduced to indicate the status of a bond, as

$$\mu(\boldsymbol{\xi}, t) = \begin{cases} 1, (s - \alpha T_{avg}) < s_0 \\ 0, (s - \alpha T_{avg}) \geq s_0 \end{cases} \tag{4}$$

Local damage parameter is introduced in order to represent the damage level as

$$\varphi(\mathbf{x}, t) = 1 - \frac{\int_H \mu(\boldsymbol{\xi}, t) dV}{\int_H dV} \tag{5}$$

PD Mechanical Laminate Model

Later on, Oterkus and Madenci (Madenci and Oterkus, 2014; Oterkus and Madenci, 2012) extended the PD theory to be applied in laminate modelling. A composite lamina can modelled as a two-dimensional structure, as shown Fig. 2. The directional dependence property can be taken into consideration by considering two bonds: the fibre bonds (shown in dashed line) and the matrix bonds (shown in straight line). In addition, the fibre direction is denoted by Φ.

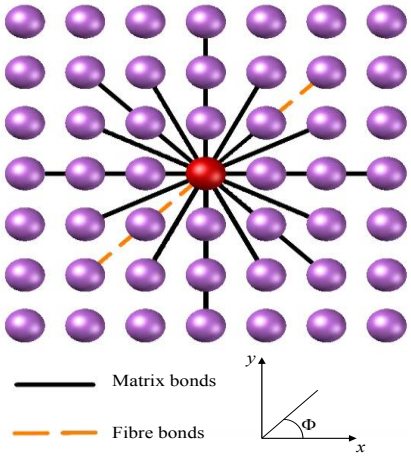

Fig. 2 PD lamina model

The bond constants for fibre and matrix bonds are denoted as c_f and c_m, respectively. The PD bond constants are expressed as (Oterkus and Madenci, 2012)

$$c_f = \frac{2E_1(E_1 - E_2)}{\left(E_1 - \frac{1}{9}E_2\right)\left(\sum_{q=1}^{Q}\xi_{qi}V_q\right)} \tag{6}$$

$$c_m = \frac{8E_1E_2}{\left(E_1 - \frac{1}{9}E_2\right)\pi h\delta^3} \tag{7}$$

where E_1 and E_2 represent the elastic modulus of a lamina in fibre and transverse directions, h represents the thickness of the lamina. V represents the volume of the material point and q represents the family member of node i. PD force is expressed as (Oterkus and Madenci, 2012)

$$\mathbf{f} = \begin{cases} (c_f + c_m)(s - \alpha_1 T)\dfrac{\boldsymbol{\eta}+\boldsymbol{\xi}}{|\boldsymbol{\eta}+\boldsymbol{\xi}|} & if\ \theta = \Phi \\ c_m(s - \alpha_\theta T)\dfrac{\boldsymbol{\eta}+\boldsymbol{\xi}}{|\boldsymbol{\eta}+\boldsymbol{\xi}|} & if\ \theta \neq \Phi \end{cases} \tag{8}$$

In the above definition, θ represents the bond direction. Because of the directional dependency of the material property, the thermal expansion coefficient in different directions varies with the bond angle. α_1 is the thermal expansion coefficient in the fibre direction, α_θ is the thermal expansion coefficient in other directions (Oterkus, 2010).

Peridynamic formulation of a composite lamina is further extended to a composite laminate (Oterkus, 2010). A laminate constitutes of multi-layer lamina with different material properties and particular stacking sequences. As a result, two types of interlayer bonds are added in the laminate model, as illustrated in Fig. 3. It is assumed that one point interacts with other points only in adjacent plies through interlayer normal bonds and interlayer shear bonds. Therefore, the horizon for interlayer normal bonds, δ_n, is the thickness of a lamina. The horizon of interlayer shear bonds, δ_s, is defined as $\delta_s = \sqrt{(\delta_n^2 + \delta^2)}$.

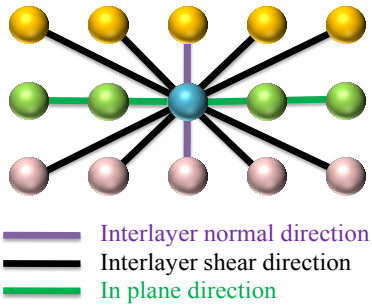

Fig. 3 PD laminate model

Interlayer normal and shear bonds are denoted as c_n and c_s, respectively. The relationships between the interlayer PD parameters and the engineering material constants are provided as (Oterkus and Madenci, 2012)

$$c_n = \frac{E_m}{hV} \tag{9}$$

$$c_s = \frac{2G_m}{\pi h}\frac{1}{\left(\delta^2 + h^2\ln\left(h^2/\delta_s^2\right)\right)} \tag{10}$$

where E_m is the elastic modulus and G_m is the shear modulus of the matrix material. The force-stretch relationship for interlayer normal and shear bonds are presented as

$$\mathbf{f}_n = c_n(s - \alpha_m T)\frac{\boldsymbol{\eta}+\boldsymbol{\xi}}{|\boldsymbol{\eta}+\boldsymbol{\xi}|} \tag{11}$$

$$\mathbf{f}_s = c_s\varphi(\Delta x)^2\frac{\boldsymbol{\eta}+\boldsymbol{\xi}}{|\boldsymbol{\eta}+\boldsymbol{\xi}|} \tag{12}$$

where φ represents shear angle of the diagonal shear bonds (Oterkus and Madenci, 2012). Δx is the spacing between material points on the plane of the lamina.

PD Thermal Laminate Model

In regard of the thermal field, the fully coupled thermomechanical PD model developed (Oterkus et al., 2014a) and extended into lamina by Oterkus and Madenci (2014) is adopted here. The heat conduction equation for a lamina is expressed as

$$\rho c_v\dot{T}(\mathbf{x},t) = \int_H\left(k\frac{\Theta(\mathbf{x}',t) - \Theta(\mathbf{x},t)}{|\boldsymbol{\xi}|} - \Theta_0\beta\dot{e}\right)dV' + \rho q_b(\mathbf{x},t) \tag{13}$$

where c_v is the specific heat capacity. Θ is the temperature and Θ_0 is the reference temperature. $T(\mathbf{x},t)$ is the temperature change of point $\mathbf{x}$ with $T(\mathbf{x},t) = \Theta(\mathbf{x},t) - \Theta_0$. Hence, $\dot{T}(\mathbf{x},t)$ is the rate of temperature change of point $\mathbf{x}$. k is called micro-conductivity. β is the PD thermal modulus. q_b is the volumetric heat source. $\dot{e}$ is the time rate of the change of stretch and its definition is shown as

$$\dot{e} = \frac{\boldsymbol{\eta}+\boldsymbol{\xi}}{|\boldsymbol{\eta}+\boldsymbol{\xi}|}\cdot\dot{\boldsymbol{\eta}} \tag{14}$$

The determinations of in-plane micro conductivity are given as (Oterkus et al., 2012)

$$k=\begin{cases}k_f+k_m, if\ \theta=\Phi\\ k_m, if\ \theta\neq\Phi\end{cases} \tag{15}$$

with

$$k_f=\frac{2(\kappa_1-\kappa_2)}{\sum_{j=1}^{N_f}|\xi|V_j} \tag{16}$$

and

$$k_m=\frac{6\kappa_2}{\pi h\delta^3} \tag{17}$$

where k_f and k_m represent the micro-conductivity in fibre and other directions. κ_1 and κ_2 are the thermal conductivities for fibre and transverse directions in the realm of classical mechanics. The heat conduction in the interlayer directions can also be represented by using Eq. 13. The interlayer thermal bond including the bonds in interlayer normal directions and interlayer shear directions can be represented as;

$$k_p=\frac{\kappa_m}{2\pi h^3(\tilde{\delta}-h)} \tag{18}$$

where κ_m is the thermal conductivity of the matrix material.

PD thermal moduli associated with the in-plane bonds can be expressed as

$$\beta=\begin{cases}\frac{1}{2}(c_f+c_m)\alpha_1, if\ \theta=\Phi\\ \frac{1}{2}c_m\alpha_\theta, if\ \theta\neq\Phi\end{cases} \tag{19}$$

For the interlayer normal and shear directions, the determinations can be expressed as

$$\beta_n=\frac{1}{2}c_n\alpha_m \tag{20}$$

$$\beta_s=\frac{1}{2}c_s\alpha_m \tag{21}$$

where α_m is the thermal expansion coefficient of the matrix material.

Failure Criteria

Because of the existing of four kinds of PD bonds in the mechanical laminate model, different critical stretch values are necessary in the following simulations. The definitions of these critical stretch values are listed as (Diyaroglu, 2016; Oterkus and Madenci, 2012; Silling and Askari, 2005)

$$s_m=\sqrt{\frac{5G_{IC}}{9K_m\delta}} \tag{22}$$

$$s_n=\sqrt{\frac{2G_{IC}}{hE_m}} \tag{23}$$

$$s_s=\sqrt{\frac{G_{IIC}}{hG_m}} \tag{24}$$

$$s_{ft}=\frac{\sigma_{1t}}{E_1} \tag{25}$$

$$s_{fc}=\frac{\sigma_{1c}}{E_1} \tag{26}$$

In the above equations, G_{IC} and G_{IIC} are the critical energy release rate for first and second failure modes, respectively. K_m, E_m, G_m are the bulk, elastic and shear modulus of the matrix material, respectively. h is the thickness of a single ply. E_1 is the longitudinal elastic modulus of a single ply. σ_{1t} and σ_{1c} are longitudinal tension and compression strength properties of the lamina. s_{ft} and s_{fc} are the critical stretch values for fibre failure in tension and compression. s_m is critical stretch related with the matrix failure in tension, indicating that the matrix bonds are only allowed to fail in tension. s_n and s_s are critical stretch values for interlayer normal bonds and interlayer shear bonds.

In conclusion, the three-dimensional laminate model formulated by PD theory is explained and will be applied in the numerical simulation in next section.

NUMERICAL SIMULATION

Problem Description

In this section, a numerical analysis is conducted for a 13-ply laminate under underwater explosive loading condition. The test plate used by LeBlanc (2011) is utilized in the simulations, illustrated in Fig. 4. The boundary region, shown in yellow colour in the figure, is clamped by six bolts. The outer radius of the plate, R_{out}, is 13.2715 cm. And the inner radius, R_{in}, is 11.43 cm. The radius of a bolt, r, is 4 mm. The plies in this laminate have the same thickness, i.e. h is 0.254 mm.

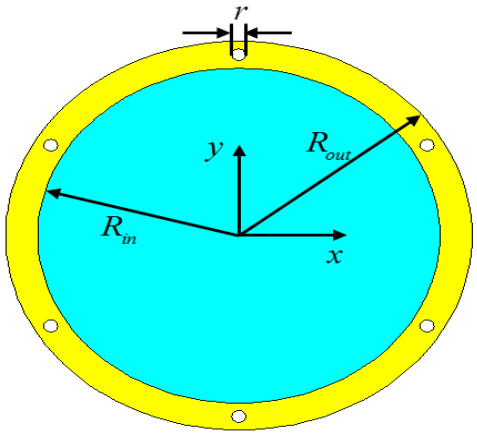

Fig. 4 Composite test plate

The material property of the laminated composite is listed in Table 1. The PD discretization of a single lamina is illustrated in Fig. 5. Each lamina has a single layer of material points with a gird sized of $\Delta x=2.6543\times10^{-3}$ m. The horizon is chosen as $\delta=3.015\Delta x$. The time step size for an explicit time integration is $\Delta t=7.69\times10^{-8}$ s. The total simulation time is set as 0.3641×10^{-3} s. As to the bond failures, the related material properties provided by Diyaroglu (2016) is adopted. The critical energy release rate for matrix failure is $G_{IC}=11.85\times10^{-3}$ MPa, thus the s_m is computed as $s_m=1.47\times10^{-2}$. The tension and compression strength properties are $\sigma_{1t}=965$ MPa and $\sigma_{1c}=-883$ MPa. The critical stretch value for fibre failure in tension

is $s_{ft}=2.46\times10^{-2}$ and the critical stretch for the fibre bond is $s_{fc}=-2.25\times10^{-2}$. As to the interlayer bonds, the critical stretch values are calculated as $s_n=7.015\times10^{-2}$ with G_{IC} being 2.73×10^{-3} MPa and $s_s=0.14$ with G_{IIC} being 7.11×10^{-3} MPa.

Table 1 Material property of the test plate

Mechanical Properties		Thermal Properties	
$E_1\,(\mathrm{GPa})$	39.3	$\alpha_1\,(\mu\mathrm{m/m/K})$	8.6
$E_2\,(\mathrm{GPa})$	9.7	$\alpha_2\,(\mu\mathrm{m/m/K})$	22.1
$G_{12}\,(\mathrm{GPa})$	3.32	$k_1\,(\mathrm{W/mK})$	10.4
Poisson's ratio ν_{12}	0.33	$k_2\,(\mathrm{W/mK})$	0.89
$\rho\,(\mathrm{kg/m^3})$	1850	$c_v\,(\mathrm{J/(kg\cdot K)})$	879
$E_m\,(\mathrm{GPa})$	3.792	$\alpha_m\,(\mu\mathrm{m/m/K})$	63
$G_m\,(\mathrm{GPa})$	1.422	$k_m\,(\mathrm{W/mK})$	0.34
Poisson's ratio ν_m	0.33	$\Theta_0\,(\mathrm{K})$	285

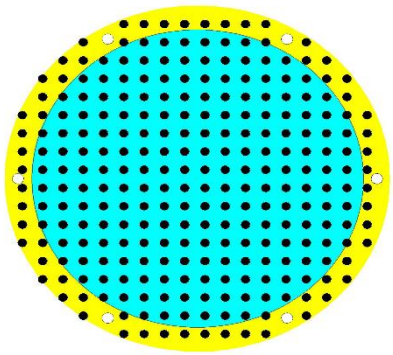

Fig. 5 PD discretization of a lamina

In respect of the determination of the shock loads, the formulation of the explosion load adopted by Diyaroglu (2016) is applied. According to the experiment conducted by LeBlanc and Shukla (2011), when the shock wave reaches the laminate, the time is set as $t=0$. Then the pressure load increases linearly to its peak value, P_{max}, during the time period $0<t\le0.04\times10^{-3}$ s. Subsequently, the pressure load retains its maximum value until 0.08×10^{-3} s. The pressure decays in an exponential form until the end of the simulation is given in Eq. 27. The peak value, P_{max}, is set to be 10.3765 MPa when the charge is located at a location of distance being 5.25 m.

$$P(t)=\begin{cases}P_{\max}\,(t/0.04)\;t<0.04\times10^{-3}\ \mathrm{s}\\ P_{\max}\;0.04\times10^{-3}\ s<t<0.08\times10^{-3}\ \mathrm{s}\\ P_{\max}\exp\left(-1000\left(t-0.08\right)/0.2\right)0.04\times10^{-3}\ s<t<1\times10^{-3}\ \mathrm{s}\end{cases} \tag{27}$$

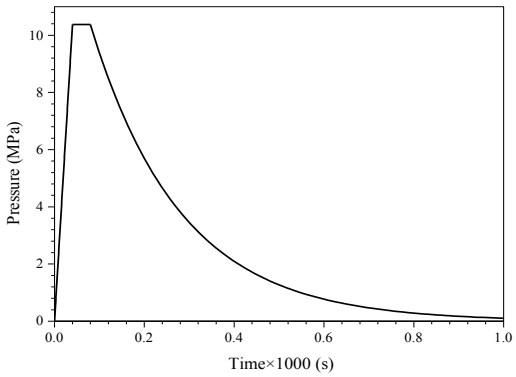

Fig. 6 Pressure load file at the test plate

The pressure distribution derived by Turken and Mecitoglu (1999) is adopted as

$$P(r)=-0.0005r^4+0.01r^3-0.0586r^2-0.001r+1 \tag{28}$$

where r represents the distance from the collective node to the centre of the test plate. Consequently, the final explosion load is defined as

$$P(r,t)=P(t)\left(-0.0005r^4+0.01r^3-0.0586r^2-0.001r+1\right) \tag{29}$$

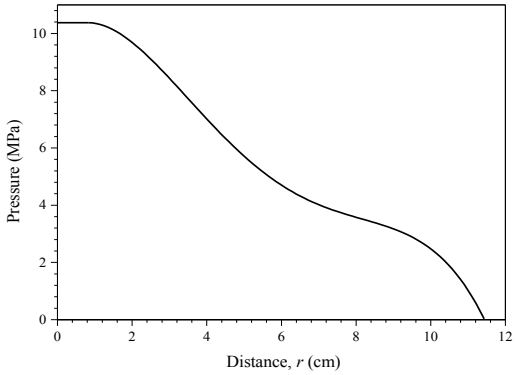

Fig. 7 Non-uniform pressure distribution over the top ply

It should be noted that only the first impact of the explosion is considered in the above load definition.

Numerical Results

First, numerical simulation without allowing failure is conducted. Uniform pressure load is applied and the supported region (shown in yellow colour) of all plies are constrained in vertical direction. All plies in the laminate experience the similar vertical (z) displacement distribution. The variation of vertical displacement of the central point in the middle ply is plotted in Fig. 8. The vertical displacement distribution of the middle ply at 0.26915×10^{-3} s is shown in Fig. 9.

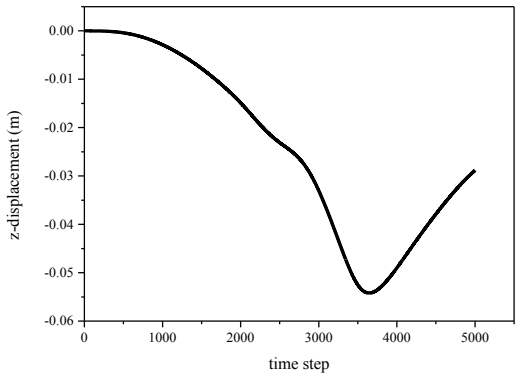

Fig. 8 Variation of the displacement in z direction of the central point

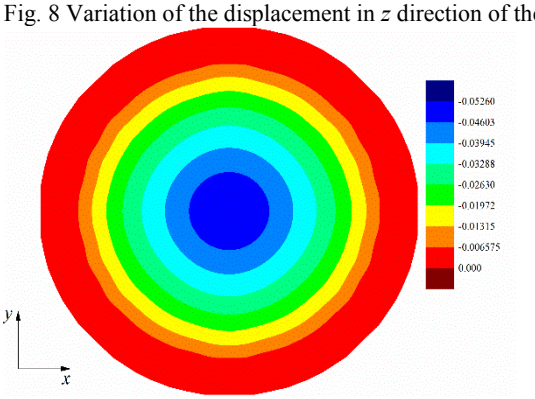

Fig. 9 Vertical displacement of the middle ply at 0.26915×10^{-3} s

Then a simulation with allowing failure is carried out under the non-uniform pressure load, $P(r,t)$. The matrix damages and temperature distributions of all plies are plotted at $t=0.26915\times10^{-3}$ s and $t=0.3461\times10^{-3}$ s in Figs. 10~11.

It can be observed that the damage patterns are different for each ply. The top ply experiences compression while the bottom ply is under tension, so the matrix damage at the bottom ply is larger than the top ply (Figs. 10~11). At the bottom ply, the regions near the holes are fragmented because of the boundary constraints. In addition, the cracks occur and propagate in the middle region due to the highest level of the non-uniform distributed pressure shock load. The cracks in the middle region mainly grow in vertical direction, which is also observed in the experiment shown in Fig. 15.

Temperature changes induced by the applied pressure shock loading, are presented for different ply locations (Figs. 10~11). Furthermore, as the time increases, the values of the temperature change increase for all 13 plies. The temperature change profiles have similar patterns with the crack damage patterns. As the top ply is under compression, temperature increases, on the other hand when the bottom ply is under tension, temperature decreases. Besides, the crack growth pattern also influences the temperature distribution. The temperature increases near the crack surfaces and decreases near the crack region. Therefore, the distribution of temperature presents a similar pattern compared with the crack pattern.

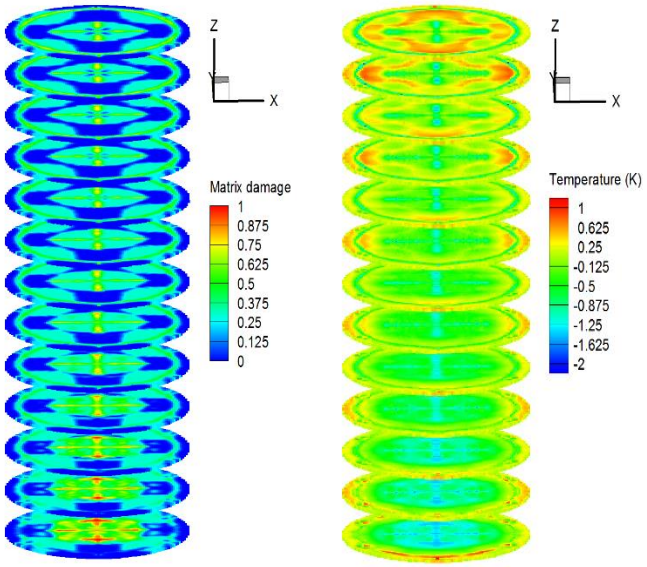

(a) (b)

Fig. 10 Matrix damage (a) and temperature distributions (b) at 0.26915×10^{-3} s

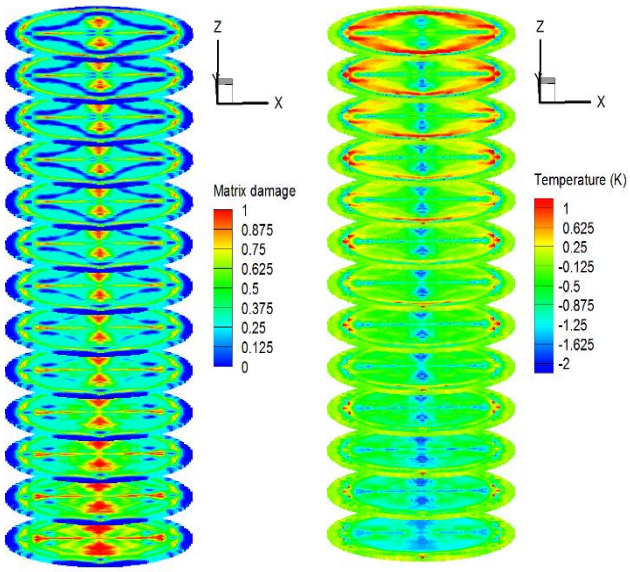

(a) (b)

Fig. 11 Matrix damage (a) and temperature distributions (b) at 0.3461×10^{-3} s

In addition to the coupled thermomechanical simulation, damage patterns for uncoupled case is also considered for comparison purposes. The comparison of the damages of the top, middle and bottom plies at $t=0.3461\times10^{-3}$ s are provided in Figs. 12~14. Different crack paths are observed from these two simulation cases, indicating the temperature effect on the damage evolution process. The region near the y axis experiences more damage in the fully coupled simulation case than the uncoupled case.

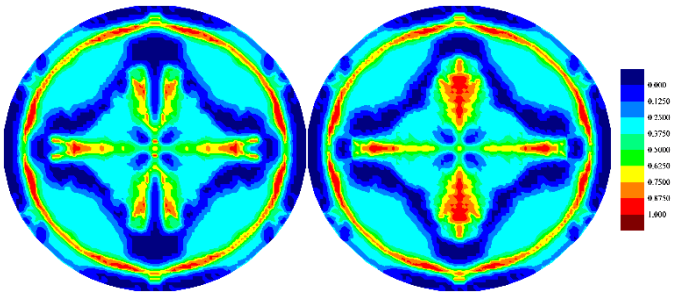

(a) (b)

Fig. 12 Matrix damage plots of top ply from uncoupled case (a) and coupled case (b) at 0.3461×10^{-3} s

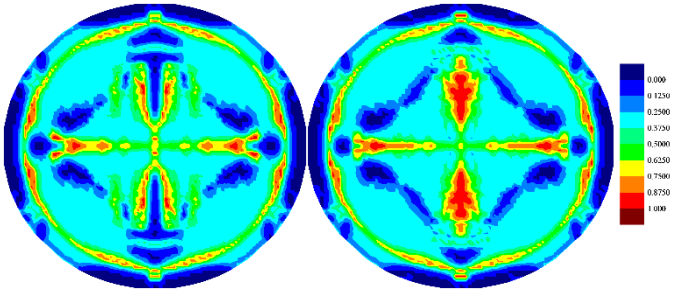

(a) (b)

Fig. 13 Matrix damage plots of middle (*7 th*) ply from uncoupled case (a) and coupled case (b) at 0.3461×10^{-3} s

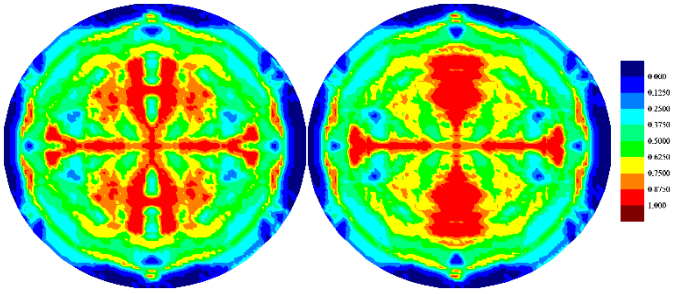

(a) (b)

Fig. 14 Matrix damage plots of bottom ply from uncoupled case (a) and coupled case (b) at 0.3461×10^{-3} s

Fig. 15 Material damage during test (LeBlanc and Shukla, 2010)

CONCLUSIONS

In this paper, a numerical analysis of a composite laminate exposed to an underwater explosion is simulated using a fully coupled peridynamic theory. A pressure shock generated by an underwater explosion is applied on the top surface of the laminate. Both the deformation and temperature change responses of the laminate are simulated. The crack propagation predictions from peridynamic theory correlate well with the experimental results, validating the capability of peridynamic theory for investigating explosion impact response of composite materials. In addition, the temperature coupling effects are studied through the comparison of the crack propagation predictions from both the uncoupled and coupled simulation cases.

ACKNOWLEDGEMENTS

The authors gratefully acknowledge financial support from China Scholarship Council (CSC No. 201506230126) and University of Strathclyde.

REFERENCE

Batra, RC, and Hassan, NM (2008). "Blast resistance of unidirectional fiber reinforced composites," *Compos Part B-eng*, 39 (3), 513-536. http://doi.org/10.1016/j.compositesb.2007.03.002

Diyaroglu, C (2016). "Peridynamics and its applications in marine structures,"

Dobyns, AL (1981). "Analysis of Simply-Supported Orthotropic Plates Subject to Static and Dynamic Loads," *Aiaa J*, 19 (5), 642-650. http://doi.org/10.2514/3.50984

Hall, DJ (1989). "Examination of the Effects of Underwater Blasts on Sandwich Composite Structures," *Compos Struct*, 11 (2), 101-120. http://doi.org/10.1016/0263-8223(89)90063-9

Kazancı, Z (2016). "A review on the response of blast loaded laminated composite plates," *Prog Aerosp Sci*, 81, 49-59. https://doi.org/10.1016/j.paerosci.2015.12.004

Khan, KA, Barello, R, Muliana, AH, and Levesque, M (2011). "Coupled heat conduction and thermal stress analyses in particulate composites," *Mech Mater*, 43 (10), 608-625. http://doi.org/10.1016/j.mechmat.2011.06.013

Kogl, M, and Gaul, L (2003). "A boundary element method for anisotropic coupled thermoelasticity," *Arch Appl Mech*, 73 (5-6), 377-398. http://doi.org/10.1007/s00419-003-0289-2

Langdon, GS, von Klemperer, CJ, Sinclair, G, and Ghoor, I (2017). *Chapter 6 - Influence of Curvature and Load Direction on the Air-Blast Response of Singly Curved Glass Fiber Reinforced Epoxy Laminate and Sandwich Panels*, Explosion Blast Response of Composites. Woodhead Publishing, pp. 133-160.

LeBlanc, J, and Shukla, A (2010). "Dynamic response and damage evolution in composite materials subjected to underwater explosive loading: An experimental and computational study," *Compos Struct*, 92 (10), 2421-2430. http://doi.org/10.1016/j.compstruct.2010.02.017

LeBlanc, J, and Shukla, A (2011). "Dynamic response of curved composite panels to underwater explosive loading: Experimental and computational comparisons," *Compos Struct*, 93 (11), 3072-3081. http://doi.org/10.1016/j.compstruct.2011.04.017

Librescu, L, and Nosier, A (1990). "Response of Laminated Composite Flat Panels to Sonic-Boom and Explosive Blast Loadings," *Aiaa J*, 28 (2), 345-352. http://doi.org/10.2514/3.10395

Librescu, L, Oh, SY, and Hohe, J (2004). "Linear and non-linear dynamic response of sandwich panels to blast loading," *Compos Part B-eng*, 35 (6-8), 673-683. http://doi.org/10.1016/j.compositesb.2003.07.003

LiVolsi, F (2014). "Response of marine composites subjected to near field blast loading."

Madenci, E, and Oterkus, E (2014). *Peridynamic theory and its applications*. Springer.

Mukherjee, N, and Sinha, PK (1996). "Thermal shocks in composite plates: A coupled thermoelastic finite element analysis," *Compos*

Struct, 34 (1), 1-12. http://doi.org/10.1016/0263-8223(95)00121-2

Oterkus, E (2010). "Peridynamic theory for modeling three-dimensional damage growth in metallic and composite structures,"

Oterkus, E, and Madenci, E (2011). "Peridynamic Theory for Damage Initiation and Growth in Composite Laminate," *Key Eng Mater*, 488-489, 355-358. http://doi.org/10.4028/www.scientific.net/KEM.488-489.355

Oterkus, E, and Madenci, E (2012). "Peridynamic Analysis of Fiber-Reinforced Composite Materials," *J Mech Mater Struct*, 7 (1), 45-84. http://doi.org/10.2140/jomms.2012.7.45

Oterkus, E, Madenci, E, Weckner, O, Silling, S, Bogert, P, and Tessler, A (2012). "Combined finite element and peridynamic analyses for predicting failure in a stiffened composite curved panel with a central slot," *Compos Struct*, 94 (3), 839-850. http://doi.org/10.1016/j.compstruct.2011.07.019

Oterkus, S, and Madenci, E (2014). "Fully coupled thermomechanical analysis of fiber reinforced composites using peridynamics," *55th AIAA/ASMe/ASCE/AHS/SC Structures, Structural Dynamics, and Materials Conference-SciTech Forum and Exposition*, Maryland,

Oterkus, S, Madenci, E, and Agwai, A (2014a). "Fully coupled peridynamic thermomechanics," *J Mech Phys Solids*, 64, 1-23. http://doi.org/10.1016/j.jmps.2013.10.011

Oterkus, S, Madenci, E, and Agwai, A (2014b). "Peridynamic thermal diffusion," *J Comput Phys*, 265, 71-96. http://doi.org/10.1016/j.jcp.2014.01.027

Rajendran, R (2008). "Reloading effects on plane plates subjected to non-contact underwater explosion," *J Mater Process Tech*, 206 (1-3), http://doi.org/275-281. 10.1016/j.jmatprotec.2007.12.022

Rajendran, R, Paik, JK, and Lee, JM (2007). "Of underwater explosion experiments on plane plates," *Exp Techniques*, 31 (1), 18-24. http://doi.org/10.1111/j.1747-1567.2007.00130.x

Ramakrishnan, M, Rajan, G, Semenova, Y, and Farrell, G (2016). "Overview of Fiber Optic Sensor Technologies for Strain/Temperature Sensing Applications in Composite Materials," *Sensors (Basel)*, 16 (1), 99. http://doi.org/10.3390/s16010099

Rao, DM, and Sinha, PK (1997). "Finite element coupled thermostructural analysis of composite beams," *Comput Struct*, 63 (3), 539-549. http://doi.org/10.1016/S0045-7949(96)00358-6

Silling, S, Weckner, O, Askari, E, and Bobaru, F (2010). "Crack nucleation in a peridynamic solid," *Int J Fracture*, 162 (1-2), 219-227. http://doi.org/10.1007/s10704-010-9447-z

Silling, SA, and Askari, E (2005). "A meshfree method based on the peridynamic model of solid mechanics," *Comput Struct*, 83 (17-18), 1526-1535. http://doi.org/10.1016/j.compstruc.2004.11.026

Silling, SA, and Bobaru, F (2005). "Peridynamic modeling of membranes and fibers," *Int J Nonlinear Mech*, 40 (2-3), 395-409. http://doi.org/10.1016/j.ijnonlinmec.2004.08.004

Silling, SA, Epton, M, Weckner, O, Xu, J, and Askari, E (2007). "Peridynamic states and constitutive modeling," *J Elasticity*, 88 (2), 151-184. http://doi.org/10.1007/s10659-007-9125-1

Turkmen, HS, and Mecitoglu, Z (1999). "Nonlinear structural response of laminated composite plates subjected to blast loading," *Aiaa J*, 37 (12), 1639-1647. http://doi.org/10.2514/3.14366